Journal of Solid State Chemistry 181 (2008) 3137–3144

Contents lists available at ScienceDirect

Journal of Solid State Chemistry

journal homepage: www.elsevier.com/locate/jssc

Sol–gel synthesis, structural and superconducting properties of $(Hg_{1-y}Se_y)Sr_2(Y_{1-x}Ca_x)Cu_2O_{6+\delta}$

E. Kandyel *

Department of Chemistry, Faculty of Science, Tanta University, Tanta 31527, Egypt

ARTICLE INFO

Article history:
Received 29 May 2008
Received in revised form
12 August 2008
Accepted 17 August 2008
Available online 23 August 2008

Keywords:
Mercury-based superconductors
Sol–gel
X-ray diffraction
Magnetic properties

ABSTRACT

A new series of Sr-based Hg-1212 superconducting cuprate $(Hg_{1-y}Se_y)Sr_2(Y_{1-x}Ca_x)Cu_2O_{6+\delta}$ ($y = 0.25$; $0.0 \leqslant x \leqslant 0.7$) have been successfully synthesized using a highly homogenous and reactive precursor $Sr_2(Y_{1-x}Ca_x)Cu_2O_z$ prepared by the citrate sol–gel process. This chemical method is fast, cheap, reproducible and more efficient than the traditional solid-state reaction method. X-ray diffraction (XRD) and Energy dispersive X-ray analyses (EDX) studies have shown that Se is required for stabilization of the Sr-based Hg-1212 phase $(Hg_{1-y}Se_y)Sr_2YCu_2O_{6+\delta}$; $y \approx 0.25$. On the other hand, electrical resistivity and magnetic susceptibility measurements indicated that substitution of Y by Ca is necessary to induce superconductivity in the 1212 $(Hg_{0.75}Se_{0.25})Sr_2(Y_{1-x}Ca_x)Cu_2O_{6+\delta}$ samples. Superconductivity is observed only for samples with $x \geqslant 0.3$ and T_c increases with increasing Ca content as well as O_2-annealing. A maximum $T_{c(onset)}$ of 85 K is found in the $(Hg_{0.75}Se_{0.25})Sr_2(Y_{0.3}Ca_{0.7})Cu_2O_{6.84}$ sample annealed in an oxygen atmosphere. The structure of O_2-annealed samples was investigated by the Rietveld refinement. For all samples, it was found that Se substitutes at the Hg site. Each Se atom is surrounded by four oxygen atoms O(3), but these are not at the ideal $(\frac{1}{2}, \frac{1}{2}, 0)$ site. Rather, these oxygen atoms are shifted along the [110] direction ((0.3989, 0.3989, 0) in the case of $x = 0.5$), implying a four-fold split site with an occupancy of 0.22(2) for each of them.

1. Introduction

The first mercury-containing cuprates discovered were the $HgBa_2RCu_2O_{6+\delta}$ phase, with R = rare-earth elements [1]. They are isostructural with a high-T_c superconductor $TlBa_2CaCu_2O_{6+\delta}$ (Tl/Ba-1212) [2], thus containing the CuO_2 layers that seem to be crucial for high-temperature superconductivity [3–4]. No diamagnetic transitions down to 12 K were detected for these phases even after oxygen treatments. Continued research by Putilin et al. [5] resulted in the discovery of the first superconducting mercury cuprate $HgBa_2CuO_{4+\delta}$ (Hg/Ba-1201) in March 1993, with $T_{c(onset)}$ up to 94 K, significantly higher than the corresponding thallium-based superconductor Tl/Ba-1201. After this discovery, the synthesis work expanded in several directions, leading to an exploration of the family of superconductors based on single-mercury oxygen layers, $HgBa_2Ca_{n-1}Cu_nO_{2n+2+\delta}$ ($n = 1$–7). The second member $HgBa_2CaCu_2O_{6+\delta}$ (Hg/Ba-1212) has $T_{c(onset)} = 127$ K [6–8]. It was shown that a rare earth containing 1212 phases is also superconducting if a heterovalent of R^{3+} replacement by Ca^{2+} is made in sufficient amounts >40% [9,10]. The homolog with $n = 3$, $HgBa_2Ca_2Cu_3O_{8+\delta}$ (Hg/Ba-1223) has a record-high $T_{c(onset)} = 135$ K [6,11,12] and 138 K in its fluorinated form [13]. Several groups have reported that its transition temperature increases up to 150–164 K under high pressure [14–17].

Although these materials possess the highest T_c value yet observed for any superconductors, they are less stable in open air as they absorb CO_2 and moisture from air and (gradually) become amorphous. It is possible that substitution of Sr for Ba would improve the chemical stability of the compounds. In fact, Ba-free high T_c cuprates (such as La–Sr–Cu–O, Bi–Sr–Ca–Cu–O, etc.) are more stable than the Ba-containing cuprates (such as Y–Ba–Cu–O, Tl–Ba–Ca–Cu–O, etc.). On the other hand, for Tl-based cuprates whose structure is similar to Hg-based cuprates, the T_c of Tl/Sr-1223 can be up to 124 K [18], which is close to that of Tl/Ba-1223 [19]. For the above reasons, more and more attention has been focused on the study of Hg/Sr-based superconducting cuprates. The Hg/Sr-based cuprates $HgSr_2Ca_{n-1}Cu_nO_{2n+2+\delta}$ have not been synthesized to date [20–27]. However, by introducing a high-valence cation M^{n+} ($n \geqslant 3$) into the Hg site, a number of Hg/Sr-based cuprates $(Hg,M)Sr_2(Ca,R)_{n-1}Cu_nO_z$ ($n = 1,2$) [20,21,24,28–42] and $(Hg,M)Sr_2(R,Ce)_2Cu_2O_z$ [43] have been synthesized inside an evacuated quartz tube. For the $n \geqslant 3$ members, $(Hg,M)Sr_2Ca_{n-1}Cu_nO_{2n+2+\delta}$ can only by synthesized under high

* Fax: +20 040 3350804.
E-mail address: skandyel@yahoo.com

0022-4596/$ - see front matter © 2008 Elsevier Inc. All rights reserved.
doi:10.1016/j.jssc.2008.08.021

pressure [27,44]. These Hg/Sr compounds were found to be chemically stable in open air and to have higher irreversibility fields compared with Hg/Ba ones [45–47].

Mercury-based cuprates are generally synthesized by the sealed quartz tube technique in a two-step process: first, by the formation of a precursor and then its mercuration. Starting with a high degree of homogenization of all precursor oxides is essential to obtain superconducting ceramics of high quality. Although sol–gel processing is a promising synthetic way to obtain better chemical homogeneity and higher reactivity of the precursor powder, only a few investigations of the application of the sol–gel technique for the synthesis of mercury-based superconductors have been reported so far. The basic idea of sol–gel is to start from a solution of cations and to transform into a gel by polymerization [48]. Drying the gel gives a xerogel that transforms to oxides upon heating. However, mercury forms insoluble compounds with many of the complex agents, such as citric or tartaric acids [49] often used in sol–gel processing cuprates. Moreover, the temperature required to transform the gel into the oxide phase is higher than the decomposition temperature of HgO at ambient pressure. For these reasons, sol–gel methods were only used for the preparation of precursor powders [49–53]. Peacock et al. [53] have investigated the formation of precursors for all three members of the homologous series $HgBa_2Ca_{n-1}Cu_nO_{2n+2+\delta}$ ($n = 1, 2, 3$) by various methods, including the sol–gel technique. They reported that it was only possible to prepare Hg/Ba-1201 by various methods, but failed when they attempted to prepare the higher Hg/Ba-1212 and Hg/Ba-1223. Kareiva and Bryntse [49] have found that only when the precursor was decomposed in vacuum it became free of carbonate, so that the Hg/Ba-1212 phase could form as a major constituent.

We have previously demonstrated that a new series of Sr-based Hg-1201 superconductor $(Hg_{1-y}Se_y)(Sr_{2-x}La_x)CuO_{4+\delta}$ with a maximum T_c of 50 K ($y = 0.25$; $x = 0.7$) can be successfully synthesized using the precursor $(Sr_{2-x}La_x)CuO_z$ prepared by the citrate sol–gel process [54]. In this paper, we report a new series of mercury-based 1212 superconductor $(Hg_{1-y}Se_y)Sr_2(Y_{1-x}Ca_x)Cu_2O_{6+\delta}$ that exhibit a maximum $T_{c(onset)}$ of 85 K.

2. Experimental

2.1. Synthesis of $Sr_2(Y_{1-x}Ca_x)Cu_2O_z$ precursor

Samples with nominal compositions $(Hg_{1-y}Se_y)Sr_2(Y_{1-x}Ca_x)Cu_2O_{6+\delta}$ ($0.0 \leqslant y \leqslant 1.0$; $0.0 \leqslant x \leqslant 1.0$) were prepared using the two-step method following the same procedure as reported in Refs. [42,54]. First, precursors with nominal composition $Sr_2(Y_{1-x}Ca_x)Cu_2O_z$ ($0.0 \leqslant x \leqslant 1.0$) were prepared by an aqueous sol–gel route using stoichiometric amounts of metal nitrates as starting materials and citric acid as the complexing agent. The dried gels were ground in an agate mortar and preheated at 500 °C for 10 h and then at 850 °C for 24 h in flowing O_2 for decomposition of carbonates with intermediate grinding. For comparison purposes, the conventional solid-state reaction (SSR) technique was also applied. We used the $Sr(CO_3)_2$, $Ca(CO_3)_2$, CuO and Y_2O_3 powders as starting substances to synthesize the precursor $Sr_2(Y_{1-x}\ Ca_x)Cu_2O_z$. The components were mixed, ground and calcinated for 24 h at a temperature of 850 °C to decompose carbonates with intermediate grinding and finally calcinating at 900 °C for another 24 h in an oxygen flow.

2.2. Synthesis of the $(Hg_{1-y}Se_y)Sr_2(Y_{1-x}Ca_x)Cu_2O_{6+\delta}$ phase

The procedure to form the $(Hg_{1-y}Se_y)Sr_2(Y_{1-x}Ca_x)Cu_2O_{6+\delta}$ phase was the same for the sol–gel-derived precursors and for the precursors from SSR. This precursor was then mixed with yellow HgO and SeO_3 in a nominal stoichiometric quantity. The resulting powder was pelletized and inserted into a quartz tube that was closed under vacuum. The samples were heated at a rate of about 3°/min up to 850 °C, held at this temperature for 10 h and then cooled down to room temperature inside the furnace.

2.3. Characterization of the samples

After heat treatment, part of the pellet was reground to perform powder X-ray measurements, and the rest was sliced into 1 mm thick rectangular bars for further characterization. The crystal structures of the samples were examined by powder X-ray diffraction (XRD) using Ni-filtered Cu$K\alpha$ radiation. A step scan mode was employed with a 2θ angular increment at 0.02° and a counting time of 10 s in the range of $5^\circ \leqslant 2\theta \leqslant 120^\circ$. The XRD data were analyzed by the Rietveld refinement program RIETAIN-94 provided by Kim and Izumi [55]. Energy-dispersive X-ray analyses (EDX) were carried out at 15 different points for some selected samples using a scanning electron microscope (SEM) (JSM-840) operated at an acceleration voltage of 25 kV and the ZAF quantitative analysis program. Superconductivity transitions were determined from measurements of both electrical resistivity and Meissner diamagnetic susceptibility as a function of temperature. A computer-controlled four-probe system with a closed-cycle He refrigerator was used for the electrical resistivity measurements. The electrical contacts to the sample were made by fine copper wires with a conductive silver paint; the current applied was 10 mA. The temperature was recorded using a calibrated Pt sensor located close to the sample. The magnetic susceptibility was measured between 100 and 5 K in the "field-cooling" mode using a superconducting quantum interference device magnetometer. The field was set at $H = 5$ Oe throughout the measurement. The measured magnetic moment (emu) was divided by the weight of the sample to yield mass magnetization, M (emu/g), which was plotted as a function of temperature.

3. Results and discussion

3.1. XRD and EDX analysis

Under the experimental conditions described earlier, the synthesis of a Hg-based oxide was carried out in two steps. First, a balance of the cations Hg/Se was performed according to the formula $(Hg_{1-y}Se_y)Sr_2(Y_{1-x}Ca_x)Cu_2O_{6+\delta}$; ($0.0 \leqslant y \leqslant 1.0$), in order to determine the average metal ratio at the Hg site. From the XRD patterns, the 1212 phase of $(Hg_{1-y}Se_y)Sr_2YCu_2O_{6+\delta}$ can be obtained only when $y > 0.2$. For $y < 0.2$, the samples are multi-phase. EDX analysis performed on different samples with $y > 0.2$ showed that the ratio remained almost constant with Hg/Se ≈ 3 and the Hg/Sr ratio is close to 0.4. The results indicate the importance of Se in the stabilization of the Sr-based Hg-1212 structure. In the second step, the Hg/Se concentration was then fixed at 0.75/0.25 and the Y/Ca ratio was varied to obtain $(Hg_{0.75}Se_{0.25})Sr_2(Y_{1-x}Ca_x)Cu_2O_{6+\delta}$. Following this, we synthesized a series of samples for $x = 0$ to 1.0. Almost single-phased samples can be obtained up to $x = 0.7$, whereas samples with $x \geqslant 0.8$ resulted in the formation of (Sr,Ca)CuO_2 and CuO as impurity phases besides the main "1212" phase, suggesting a solubility limit of Ca at the Y site of around 0.7. For the sample with $x = 1.0$, the diffraction peaks of the 1212 phase were hardly observable, indicating that yttrium is also necessary for the formation of the (Hg,Se)-1212 phase. The structural and superconducting parameters for $(Hg_{0.75}Se_{0.25})Sr_2(Y_{1-x}Ca_x)Cu_2O_{6+\delta}$ series are

Table 1
Nominal composition, structural and superconducting properties of Sr-based Hg-1212 $(Hg_{0.75}Se_{0.25})Sr_2(Y_{1-x}Ca_x)Cu_2O_{6+\delta}$ superconducting cuprates

x	a (Å)	c (Å)	As-prepared		O_2-annealed	
			$T_{c(onset)}$ (K)	$T_{c(zero)}$ (K)	$T_{c(onset)}$ (K)	$T_{c(zero)}$ (K)
0.0	3.8224(4)	11.8118(3)	–	–	–	–
0.1	3.8205(4)	11.8227(2)	–	–	–	–
0.2	3.8189(2)	11.8312(5)	–	–	–	–
0.3	3.8169(1)	11.8425(1)	41	–	50	27
0.4	3.8153(3)	11.8521(1)	48	20	59	41
0.5	3.8134(1)	11.8640(3)	57	36	67	49
0.6	3.8116(4)	11.8757(2)	68	50	77	62
0.7	3.8101(3)	11.8849(2)	75	60	85	78
0.8	3.8109(5)	11.8877(7)	70	48	76	54

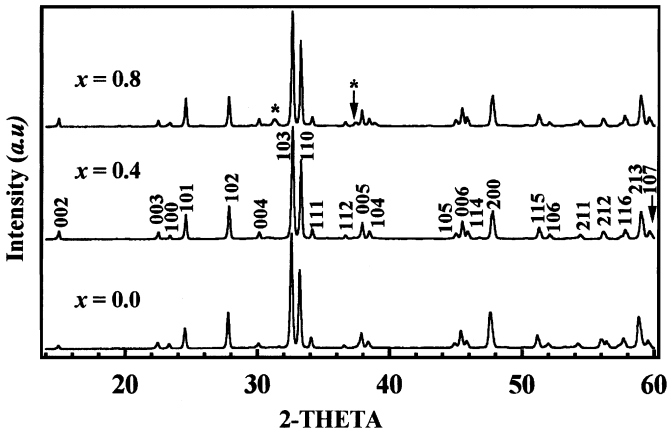

Fig. 1. X-ray powder diffraction patterns for $(Hg_{0.75}Se_{0.25})Sr_2(Y_{1-x}Ca_x)Cu_2O_{6+\delta}$ samples with $x = 0.0$, 0.4 and 0.8. Indexed peaks correspond to a Sr-based (Hg,Se) -1212 phase and impurity peaks are labeled by asterisks.

summarized in Table 1. Powder XRD patterns of some selected samples are shown in Fig. 1. Almost all the diffraction peaks for the samples with $x<0.8$ can be indexed according to the tetragonal structure following the $P4/mmm$ space group.

EDX analysis was performed on numerous crystals of samples with nominal composition $(Hg_{0.75}Se_{0.25})Sr_2(Y_{1-x}Ca_x)Cu_2O_{6+\delta}$ ($x = 0.0$–0.7) to verify the calcium composition. The results shown in Fig. 2 indicate that the Hg, Se, Sr and Cu contents are almost constant; Hg/Se ≈ 3 and Sr/Cu ≈ 1.0 whatever the crystals In contrast, the calcium and yttrium contents vary significantly, but are correlated to each other, i.e., from "$Y_{1.0}Ca_{0.0}$" to "$Y_{0.3}Ca_{0.7}$." According to the obtained results, we can speculate that actually selenium occupies the mercury sites and does not enter copper positions during the formation of the Hg/Sr-1212 superconducting phase. Moreover, the Ca content in the main phase actually increases corresponding to the nominal Ca composition x.

The variation of the tetragonal lattice parameters a and c with x in $(Hg_{0.75}Se_{0.25})Sr_2(Y_{1-x}Ca_x)Cu_2O_{6+\delta}$ is shown in Fig. 3. Note that the lattice parameter a decreases with increasing x whereas lattice parameter c shows the opposite behavior. We propose that the larger contraction in a with increasing x in $(Hg_{0.75}Se_{0.25})Sr_2(Y_{1-x}Ca_x)Cu_2O_{6+\delta}$ could be considered to be due to an increase in the average copper oxidation state arising from the substitution of low-valence Ca^{2+} for high-valence Y^{3+}, which in turn leads to shorter Cu–O distances within the copper oxygen sheets. The increase in c with Ca is attributable to the expansion of a ((Ca,Y)O_8) coordination polyhedron with a tetragonal prism form because the effective ionic radius, r, in the eight-fold coordination

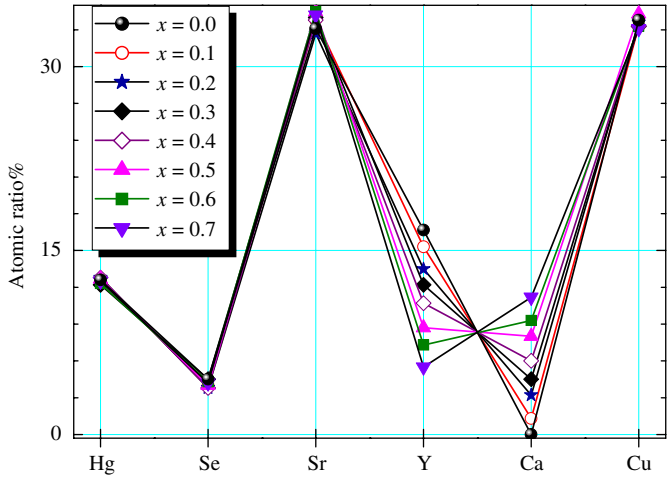

Fig. 2. Atomic percentage of $(Hg_{0.75}Se_{0.25})Sr_2(Y_{1-x}Ca_x)Cu_2O_{6+\delta}$ ($x = 0.0$–0.7) from EDX analysis.

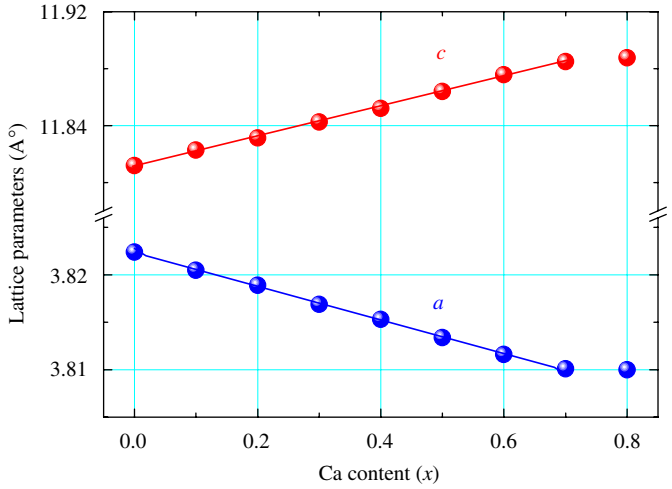

Fig. 3. Ca-content dependence of the tetragonal lattice parameters a and c for $(Hg_{0.75}Se_{0.25})Sr_2(Y_{1-x}Ca_x)Cu_2O_{6+\delta}$.

of Ca^{2+} ($r = 1.12$ Å) is larger than that of Y^{3+} ($r = 1.019$ Å) [56]. Such a behavior is observed for other 1212-type layered cuprates, (Hg,M)$Sr_2(R_{1-x}Ca_x)Cu_2O_{6+\delta}$ [20–24,34–42] and (Tl,M)$Sr_2(R_{1-x}Ca_x)Cu_2O_z$ [57], when the rare earth is substituted by Ca.

3.2. Structure refinement

Refinements of the structure of $(Hg_{0.75}Se_{0.25})Sr_2(Y_{1-x}Ca_x)Cu_2O_{6+\delta}$ ($x = 0.0$, 0.3, 0.5 and 0.7) samples from X-ray powder diffraction data were carried out assuming the symmetry of space group $P4/mmm$ and using Hg-1212 as the starting model in which (Hg,Se) ions occupy the crystallographic 1a site (0, 0, 0), Y/Ca the 1d site $(\frac{1}{2},\frac{1}{2},\frac{1}{2})$, Sr ions the 2$h$ site $(\frac{1}{2},\frac{1}{2},z;\ z\approx0.21)$, Cu the 2$g$ position (0, 0, z; $z\approx0.36$), O(1) in 4i $(\frac{1}{2},0,z;\ z\approx0.37)$, O(2) in 2$g$ (0, 0, z; $z\approx0.16$) and O(3) in the 1c $(\frac{1}{2},\frac{1}{2},0)$ position, respectively. Since Hg and Se atoms as well as Y and Ca atoms are considered to be statistically distributed over the same sites, their occupancies (g) and isotropic thermal parameters (B-iso) were constrained as follows: $g_{Hg}+g_{Se}=1$, $g_Y+g_{Ca}=1$, $B_{Hg}=B_{Se}$ and $B_Y=B_{Ca}$. The isotropic thermal parameters (B-iso) of the anions were kept fixed at 1 Å^2. Because all samples showed similar behavior in the least

square refinements, the same procedures given below were applied for all samples. At the first step of the refinement, the scale factor, background parameters, zero point, lattice parameters and peak shape parameters were refined. In the second step, along with the above parameters, the positional (x, y, z), thermal and occupancy parameters were varied. In the initial refinements, it was found that Sr, Cu, O(1) and O(2) sites were fully occupied within the error bars. In the subsequent refinements, therefore, the occupancies of those sites were fixed at unity in order to achieve the maximum sensitivity for other refined parameters, while g for O(3), which is the oxygen site on the (Hg,Se)O_δ layer, was refined. The occupancy of each site was checked again after final refinements. The stoichiometry of the (Hg,Se)-1212 samples, determined from the Rietveld refinements, is close to that observed by X-ray microanalysis in SEM. The refined amount of Se on the Hg site is not significantly different, around 25%. Moreover, the Y/Ca refined ratio is close to the nominal ones. This result is in agreement with EDX microanalysis.

The structural parameters which were assumed initially led to a good fit with reasonable structural parameters, but other possible models, which incorporate displacement and deficiencies for other atomic sites, were tested. In one of these attempts, the O(3) is shifted from a high symmetry position 1c ($\frac{1}{2},\frac{1}{2},0$) to a four-fold split site 4j (x, x, 0) or 4n (x,$\frac{1}{2}$,0) or 8p (x, y, 0) or the general position 16u (x, y, z). For all samples, the former choice gave a better fit with O(3) shifted along the [110] direction ((0.3989, 0.3989, 0) in the case of $x = 0.5$), implying a four-fold split site with an occupancy of 0.22(2) for each of them. Obviously, the size mismatch between (Hg,Se)O and perovskite layers leaves a lot of extra space for O(3) at the centre of the (Hg,Se)O square. Displacements of O(3) from the ideal ($\frac{1}{2},\frac{1}{2},0$) location have been observed in a number of Sr-based Hg-1201 and Hg-1212 structures, e.g., $Hg_{0.7}V_{0.3}Sr_{1.8}La_{0.2}CuO_{4+\delta}$ [32], $(Hg_{0.7}Cr_{0.3})Sr_2CuO_{4+\delta}$ [46], $(Hg_{1-x}Re_x)Sr_2CaCu_2O_{6+\delta}$ [47] and $(Hg_{0.7}Mo_{0.3})Sr_2(Ca_{0.5}Nd_{0.5})Cu_2O_{6+\delta}$ [39]. The occupancy of this site (δ) was as large as 0.82 in $Hg_{0.7}V_{0.3}Sr_{1.8}La_{0.2}CuO_{4+\delta}$ [32], 0.88 in $Hg_{1-x}Cr_xSr_2CuO_{4+\delta}$ [46], 1.0 in $(Hg_{0.75}Re_{0.25})Sr_2CaCu_2O_{6+\delta}$ [47], 1.0 in $(Hg_{0.7}Mo_{0.3})Sr_2(Ca_{0.5}Nd_{0.5})Cu_2O_{6+\delta}$ [39] and 0.88 in $(Hg_{0.75}Se_{0.25})Sr_2(Y_{0.5}Ca_{0.5})Cu_2O_{6+\delta}$ in sharp contrast with $\delta = 0.06$ and 0.22 for $HgBa_2CuO_{4+\delta}$ and $HgBa_2CaCu_2O_{6+\delta}$, respectively. However, the higher values of δ in these Sr-based cuprates are expected due to the presence of higher valence V, Cr, Mo, Re and Se ions in the place of the Hg ions in the structure. Partial substitution of V^{5+}, Cr^{6+}, Mo^{6+}, Re^{7+} and Se^{6+} at Hg^{2+} sites is bound to induct more

Table 2
Crystallographic data for O_2-annealed $(Hg_{0.75}Se_{0.25})Sr_2(Y_{1-x}Ca_x)Cu_2O_{6+\delta}$ samples (space group $P4/mmm$)

x		0.0	0.3	0.5	0.7
a (Å)		3.8224(4)	3.8169(1)	3.8134(1)	3.8101(3)
c (Å)		11.8118(3)	11.8425(1)	11.8640(3)	11.8849(2)
R_{wp} (weighted pattern R-factor) (%)		6.41	6.64	6.55	7.94
R_I (integrated intensity R-factor) (%)		3.34	4.05	3.06	3.36
R_P (pattern R-factor) (%)		4.59	4.49	3.42	4.72
R_e (expected R-factor) (%)		3.37	3.69	3.97	4.01
S (R_{wp}/R_e) (%)		1.90	1.80	1.65	1.98
Hg/Se	1a				
	g	0.73/0.27(3)	0.77/0.23(3)	0.76/0.24(3)	0.75/0.25(5)
	x,y,z	0	0	0	0
	B_iso (Å^2)	0.7(2)	0.6(3)	0.7(1)	0.5(1)
Sr	2h				
	g	1	1	1	1
	x,y	$\frac{1}{2}$	$\frac{1}{2}$	$\frac{1}{2}$	$\frac{1}{2}$
	z	0.2093(4)	0.2095(3)	0.2095(4)	0.2095(4)
	B_iso (Å^2)	0.2(2)	0.5(3)	0.3(2)	0.14(7)
Ca/Y	1d				
	g	0.00/0.98(2)	0.27/0.73(4)	0.48/0.52(3)	0.64/0.36(9)
	x,y,z	$\frac{1}{2}$	$\frac{1}{2}$	$\frac{1}{2}$	$\frac{1}{2}$
	B_iso (Å^2)	0.28(3)	0.2(2)	0.27(2)	0.3(1)
Cu	2g				
	g	1	1	1	1
	x,y	0	0	0	0
	Z	0.3586(6)	0.3605(4)	0.3595(6)	0.3619(7)
	B_iso (Å^2)	0.14(5)	0.4(1)	0.22(3)	0.22(2)
O(1)	4i				
	g	1	1	1	1
	x	$\frac{1}{2}$	$\frac{1}{2}$	$\frac{1}{2}$	$\frac{1}{2}$
	y	0	0	0	0
	z	0.3686(5)	0.3686(5)	0.3685(7)	0.3723(2)
	B_iso (Å^2)	1.0	1.0	1.0	1.0
O(2)	2g				
	g	1	1	1	1
	x,y	0	0	0	0
	z	0.173(3)	0.174(4)	0.173(4)	0.173(3)
	B_iso (Å^2)	1.0	1.0	1.0	1.0
O(3)	4j				
	g	0.25(4)	0.23(5)	0.22(2)	0.21(4)
	x,y	0.4077(3)	0.4045(6)	0.3989(7)	0.3869(6)
	z	0	0	0	0
	B_iso (Å^2)	1.0	1.0	1.0	1.0

oxygen in the lattice, and it is not surprising that a lot of this excess oxygen occupies the O(3) site. The disorder of O(3) ions has often been accompanied by a disorder of Cr and V ions in the case of Sr-based (Hg,Cr)-1201 [46] and (Hg,V)-1212 [58] structures. Thus, some additional refinements involving the displacements or splits of (Hg,Se) ions were carried out as follows:

(1) Hg/Se atoms were displaced from the ideal 1*a* (0, 0, 0) site to the (*x*, *x*, 0) or (*x*, 0, 0) position. But the magnitudes of the displacements were too small (~0.063 Å) to assign the shifted positions of these atoms.
(2) Keeping the Hg atom fixed at the (0, 0, 0) site, the Se atom was shifted in the [100] or the [110] direction. However, these refinements did not improve the fit. On the other hand, Hyatt et al. were able to displace the V atom in $(Hg_{0.65}V_{0.35})Sr_2(Nd_{0.6}Sr_{0.4})Cu_2O_{6+\delta}$ [58] to the position (0.12, 0, 0) and split the O(2) site into two sites: one is the original 2 g site at (0, 0, 0.164) and the other is the O(2)' 8*s* site at (0.05, 0, 0.126) with a fair occupancy (0.8) at the new O(2)' site whereas our XRD structural refinements on $(Hg_{0.75}Se_{0.25})Sr_2(Y_{1-x}Ca_x)Cu_2O_{6+\delta}$ did not support any displacement of the Se atom or splitting of the O(2) site.

The final structural parameters are listed in Table 2. For an example of the refinement result, Fig. 4 shows the observed and calculated XRD patterns for $(Hg_{0.75}Se_{0.25})Sr_2(Y_{0.5}Ca_{0.5})Cu_2O_{6+\delta}$, where a good agreement was obtained between the observed and the calculated patterns. Crosses show raw diffraction data and the solid line overlying them represents the calculated pattern. Vertical markers below the diffraction pattern indicate the allowed Bragg reflections for (Hg,Se)-1212, and Δy indicates the difference between observed and calculated intensities on the same scale, where the *R*-factors indicate that the assigned structure model is correct. Table 3 gives the selected metal–oxygen interatomic distances and bond angle.

All the distances agree well with those observed in (Hg,*M*)-1212 and other cuprate superconductors. Each Cu atom is coordinated to four O(1) atoms firmly and one apical O(2) atom additionally, forming an elongated tetragonal pyramid (Fig. 5). This geometric configuration displays a typical feature of the coordination for Cu in superconducting copper oxides. Each Hg/Se atom has two short and opposing Hg/Se–O(2) bonds parallel to the *c*-axis (Fig. 5) and four Hg/Se–O(3). It can be seen that the $Hg/Se–O_{apical}$ distances decrease with increasing Ca concentration but not as much as the $Cu–O_{apical}$ distances increase. The latter increases from 2.146(4) to 2.623(6) Å, and this yields noticeable elongation of the *c*-axis with increasing Ca concentration

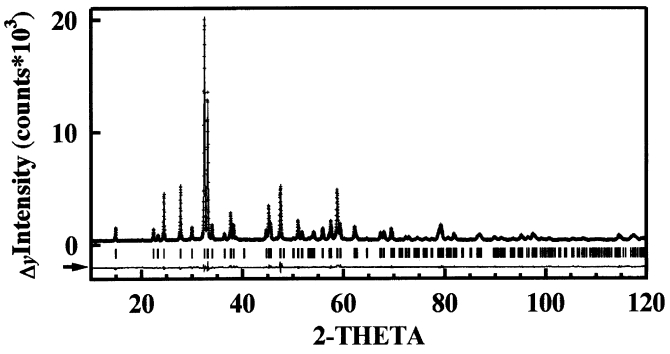

Fig. 4. The Rietveld refinement pattern for O_2-annealed $(Hg_{0.75}Se_{0.25})Sr_2(Y_{0.5}Ca_{0.5})Cu_2O_{6+\delta}$. Crosses show raw diffraction data and the solid line overlying them shows the calculated pattern. Vertical markers below the diffraction pattern indicate the allowed Bragg reflections for (Hg,Se)-1212, and Δy indicates the difference between observed and calculated intensities on the same scale.

Table 3
Selected metal–oxygen distances, number of equivalent bonds (*N*) and bond angle in O_2-annealed $(Hg_{0.75}Se_{0.25})Sr_2(Y_{1-x}Ca_x)Cu_2O_{6+\delta}$

	N	$x = 0.0$	0.3	0.5	0.7
Selected interatomic distances (Å)					
Hg/Se–O(2)	2	2.109(7)	2.088(3)	2.065(2)	2.044(5)
Hg/Se–O(3)	4	2.702(5)	2.759(8)	2.691(4)	2.766(3)
Sr–O(1)	4	2.718(2)	2.702(1)	2.749(3)	2.712(6)
Sr–O(2)	4	2.752(2)	2.738(4)	2.731(3)	2.732(5)
Sr–O(3)	1	2.409(1)	2.557(7)	2.514(4)	2.566(2)
Y/Ca–O(1)	8	2.405(5)	2.417(3)	2.428(3)	2.442(4)
Cu–O(1)	4	1.953(2)	1.937(3)	1.925(5)	1.911(2)
Cu–O(2)	1	2.146(6)	2.228(3)	2.462(2)	2.623(6)
Selected bond angle (deg)					
O(1)–Cu–O(1)		167(3)	173(3)	175(3)	176(4)

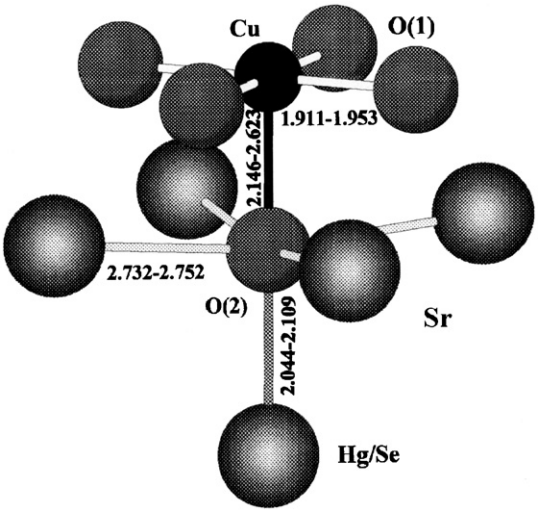

Fig. 5. Atomic configuration around an O(2) atom. Numbers attached to some bonds denote their lengths. O(3) atoms are not drawn.

(see Fig. 3). In the Ca-free 1212 structure, the CuO_2 layers are more distorted than in Ca-containing samples, which can be ascribed to interaction between atoms in the CuO_2 layers and the layers with (Y,Ca) cations. An increase of the Y concentration (with smaller ionic size) leads to an increased repulsion of the copper ions and this leads to a shift of the copper atoms towards the apical oxygen atoms in the SrO layers. In addition, the bond between Y/Ca and oxygen in the CuO_2 layers becomes stronger when the amount of Y increases. These structural peculiarities result in a puckering of the CuO_2 layer. As seen from the angles in Table 3, this layer is most distorted in the structure of $(Hg_{0.75}Se_{0.25})Sr_2YCu_2O_{6+\delta}$. The puckering in the present 1212 structure results in a significant elongation of the in-plane CuO distance, which may be the reason for the absence of superconductivity in the Ca-free sample.

3.3. Superconducting properties

Fig. 6 shows the temperature dependence of electrical resistivity for a series of as-synthesized samples of $(Hg_{0.75}Se_{0.25})Sr_2(Y_{1-x}Ca_x)Cu_2O_{6+\delta}$. The as-prepared samples with $x = 0.0$–0.2 exhibit only semiconducting behavior in the whole temperature range above 10 K. As the calcium content *x* increases to 0.3, superconductivity appears, both the superconducting onset temperature $T_{c(onset)}$ and the zero-resistivity temperature $T_{c(zero)}$

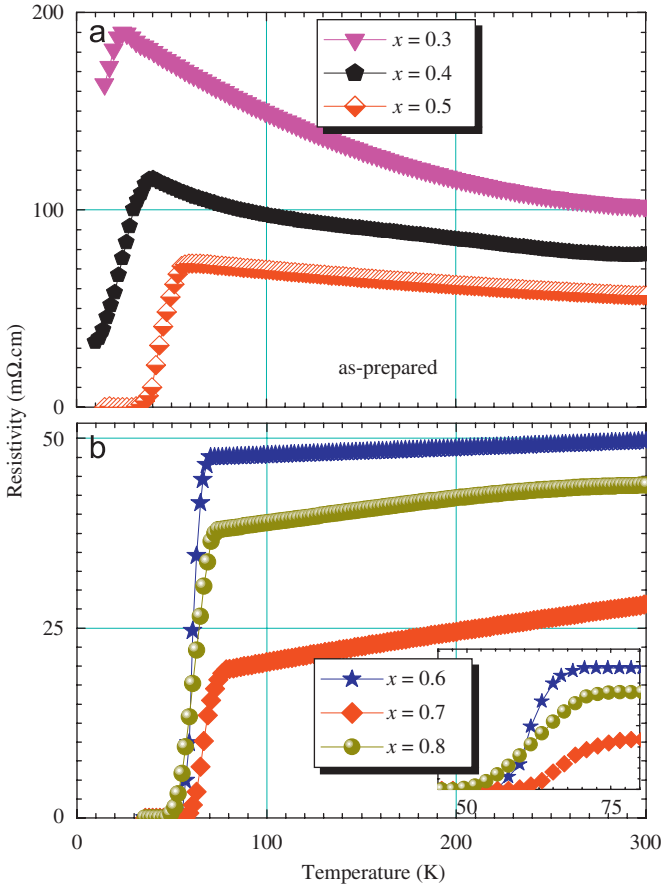

Fig. 6. Temperature dependence of electrical resistivity for as-prepared $(Hg_{0.75}Se_{0.25})Sr_2(Y_{1-x}Ca_x)Cu_2O_{6+\delta}$ samples: (a) $x = 0.3$–0.5 and (b) $x = 0.6$–0.8.

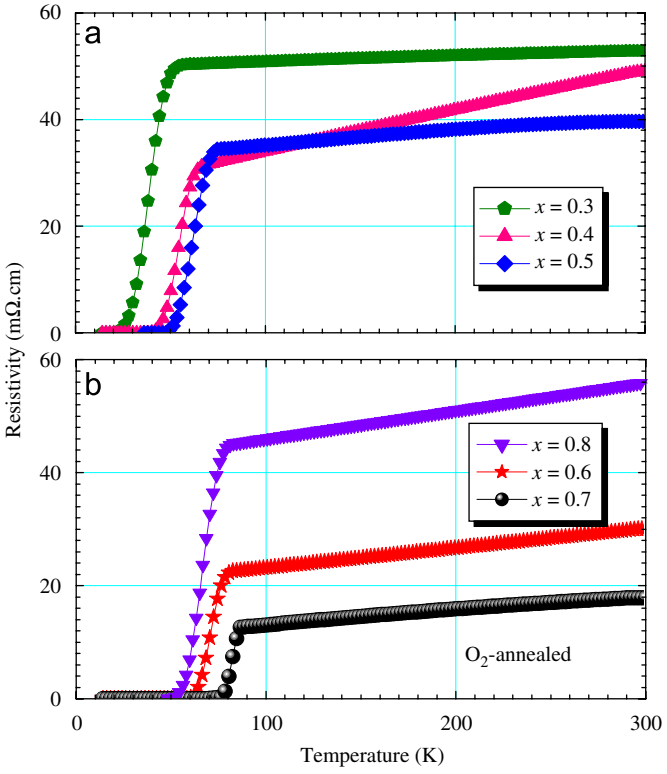

Fig. 7. Temperature dependence of electrical resistivity for O_2-annealed $(Hg_{0.75}Se_{0.25})Sr_2(Y_{1-x}\ Ca_x)Cu_2O_{6+\delta}$ samples: (a) $x = 0.3$–0.5 and (b) $x = 0.6$–0.8.

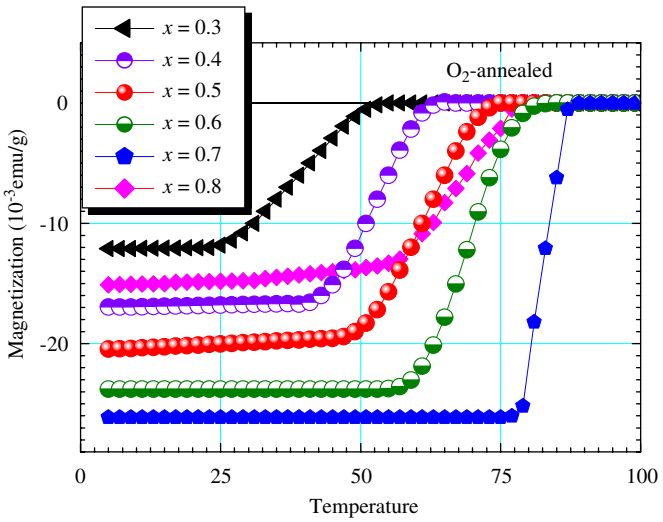

Fig. 8. Temperature dependence of the magnetic susceptibility obtained in field-cooled measurements for O_2-annealed $(Hg_{0.75}Se_{0.25})Sr_2(Y_{1-x}Ca_x)Cu_2O_{6+\delta}$ with $x = 0.3$–0.8.

increase and the normal state resistivity at $T_{c(onset)}$ decreases. However, as the Ca content increases further above 0.7, both $T_{c(onset)}$ and $T_{c(zero)}$ begin to decrease again as is seen for the sample with $x = 0.8$. The decrease of the $T_{c(zero)}$ is also accompanied by an increase of the normal state resistivity. This result indicates that the best-quality samples can be obtained from $x = 0.3$–0.7. In an attempt to improve the superconducting behavior or to induce superconductivity in the as-sintered $(Hg_{0.75}Se_{0.25})Sr_2(Y_{1-x}Ca_x)Cu_2O_{6+\delta}$, the samples were annealed at 350 °C in flowing oxygen and furnace cooled to room temperature. The XRD patterns did not show any observable change after the treatment. Fig. 7 shows the temperature dependence of electrical resistivity for the O_2-annealed samples. After the heat treatment, we could not observe the superconductivity for the samples with a low Ca content ($x<0.3$), while the superconductivity of the samples with $x \geqslant 0.3$ is largely enhanced. All the samples with $x \geqslant 0.3$ exhibit metallic behavior in the normal state with a $T_{c(onset)}$ of 50, 59, 67, 77, 85 and 76 K and a $T_{c(zero)}$ of 27, 41, 49, 62, 78 and 54 for the samples with $x = 0.3$, 0.4, 0.5, 0.6, 0.7 and 0.8, respectively.

The temperature dependence of dc-magnetic susceptibility for the O_2-annealed samples with $x = 0.3$–0.8 measured under a field-cooling condition of 5 Oe is shown in Fig. 8. A one-step transition is observed for each sample, indicating the presence of only one superconducting phase in full agreement with the results of XRD (Fig. 1). The onset transition temperature coincides with T_c determined from the resistivity measurement (Fig. 7). The onset of diamagnetism appeared at 50, 59, 67, 77, 85 and 76 K for the samples with $x = 0.3$, 0.4, 0.5, 0.6, 0.7 and 0.8, respectively. The value of the superconducting (Meissner) volume fraction was calculated using the formula $(4\pi\rho M/H)100\%$, where ρ is the X-ray density of the sample in (g/cc), M the magnetization value (emu/g) at 5 K and H is the magnetic field in Oe. The Meissner volume fraction of the superconducting phase is estimated to be 20.4%, 28.5%, 34.4%, 40.0%, 43.4% and 25.4% of $-1/4\pi$, for the samples with $x = 0.3$, 0.4, 0.5, 0.6, 0.7 and 0.8, respectively, which suggests that the samples essentially showed bulk superconductivity.

Fig. 9 indicates that the superconducting transition temperature, for both as-prepared and O_2-annealed samples, increases

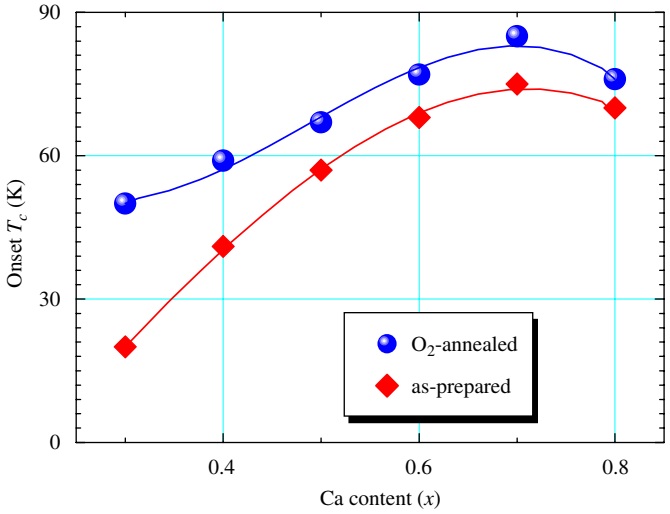

Fig. 9. Dependence of onset T_c on the Ca content for as-prepared and O_2-annealed samples of $(Hg_{0.75}Se_{0.25})Sr_2(Y_{1-x}Ca_x)Cu_2O_{6+\delta}$.

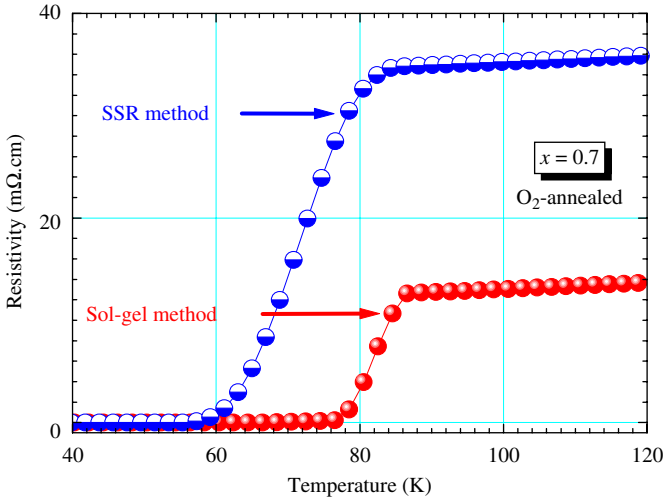

Fig. 10. Temperature dependence of electrical resistivity for O_2-annealed $(Hg_{0.75}Se_{0.25})Sr_2(Y_{0.3}Ca_{0.7})Cu_2O_{6+\delta}$ samples obtained from the sol–gel and SSR methods.

with increasing x from 0.3 to 0.7. Therefore, it suggests that the calcium content in the (Ca,Y) site as well as the oxygen content via annealing treatments are important factors in controlling the superconducting properties of the (Hg,Se)-1212 phase. The highest T_c obtained was 85 K for the sample with $x = 0.7$. It is generally accepted that the T_c of superconducting copper-oxide-based compounds depends on the density of mobile holes in the CuO_2 planes and thus on the average Cu valency. We propose that the replacement of high-valence Y^{3+} ions by the low-valence Ca^{2+} ions leads to an increase in the hole concentration in the CuO_2 sheets and enhances the T_c with increasing x in the range $0.3 \leqslant x \leqslant 0.7$. This proposal is partly supported by the observed contraction of the lattice parameter a with increasing Ca content (as shown in Fig. 3). For $x \geqslant 0.8$, the hole concentration could not be further increased, which may arise from the natural solubility limit of Ca in the Y sites. Consequently, a broadening of the superconducting transition was obtained for the $x = 0.8$ sample, perhaps due to the contribution from the impurity phase(s).

The results in Fig. 9 show that the present compounds are in the underdoped region because T_c increases with increasing x or increasing Cu valence. We evaluated the Cu valence for the O_2-annealed sample with $x = 0.5$ using the refined chemical composition $(Hg_{0.76}Se_{0.24})Sr_2(Y_{0.52}Ca_{0.48})Cu_2O_{6.88}$ by Rietveld analysis described above. Assuming the valences of Hg^{2+}, Se^{6+}, Sr^{2+}, Y^{3+}, $Ca^{2+}$and O^{2-}, we obtain a Cu valence of 2.14 from charge neutrality. This value falls in the underdoped region reported by Fukuoka et al. [59]. The oxygen content for the as-prepared sample with the same x of 0.5 was also refined as $z = 6.83(4)$ by Rietveld analysis. Although the accuracy in z is low in the X-ray structural refinement, the change in z between as-prepared and O_2-annealed samples with $\Delta z = 0.05$ corresponds to an increase of Cu valence of 0.05. Therefore, T_c for the O_2-annealed sample is higher than the as-prepared one when the sample is in the underdoped region. The effect of Δz on the Cu valence is equivalent to the change in x by an amount of $\Delta x = 2\Delta z$. Namely, the T_c–x curve for the as-prepared samples in Fig. 9 should be shifted by an amount of $\Delta x = 0.1$ to compare with the T_c–x curve for the O_2-annealed samples.

As described in Section 1, contrary to the case of Ba-based 1212-type, $HgBa_2RCu_2O_{6+\delta}$ (R = rare earths) cuprate, the Sr-based $HgSr_2RCu_2O_{6+\delta}$ cannot form due to the smaller ionic size of Sr^{2+} compared with Ba^{2+}. One way to stabilize this structure is to substitute Hg with an ion M with a smaller size forming $(Hg,M)Sr_2RCu_2O_{6+\delta}$. A smaller M ion usually has a higher valence, and thus this substitution would decrease the average Cu valence and is not helpful for superconductivity. However, such a substitution usually carries some oxygen into the structure (i.e., δ increases), resulting in an increase rather than a decrease of the average Cu valence. But this increase of charges in the CuO_2 layers is still not enough to induce superconductivity. Accordingly, further hole doping by Ca substitution for R (forming $(Hg,M)Sr_2(R,Ca)Cu_2O_{6+\delta}$) is required to make it superconducting. Since $(Hg,M)Sr_2RCu_2O_{6+\delta}$ is more O-rich, partial substitution of Ca^{2+} for R^{3+} can bring the average Cu valence up to or close to the optimal value of a superconductor. The present study confirmed the above-mentioned proposal where substituting $M = Se^{6+}$ for Hg^{2+} is required for the stabilization of the Sr-based $(Hg,Se)Sr_2YCu_2O_{6+\delta}$ and a further substitution of Ca for Y are necessary for inducing superconductivity. Another interesting point is that Hg/Sr-1212, $(Hg,M)Sr_2(R,Ca)Cu_2O_{6+\delta}$, exhibits a surprisingly lower T_c value (< 100 K) than that of the Hg/Ba-1212, $HgBa_2CaCu_2O_{6+\delta}$ phase (≈ 127 K) in spite of stabilization by Se doping. The lower T_c in Hg/Sr-1212 with the optimal hole concentration than in Hg/Ba -1212 may be relevant to the differences in the oxygen coordination and the resultant flatness of the CuO_2 layer.

Finally, it was interesting to compare the properties of superconductor ceramics obtained from a sol–gel precursor to that obtained from the conventional SSR. We found that the sol–gel route is useful in obtaining almost a single-phase superconducting Sr-based (Hg,Se)-1212 with zero resistance temperature as high as 78 K (see Fig. 10 for $x = 0.7$). The final product is so homogenous that the superconducting transition is steeper than the ceramic sample prepared by the SSR method. Moreover, sol–gel processing is efficient, not only to prepare better superconducting ceramics but also to save annealing time treatments during precursor synthesis.

4. Conclusion

In the present study, we have prepared a new series of Sr-based (Hg,Se)-1212 cuprates, $(Hg_{0.75}Se_{0.25})Sr_2(Y_{1-x}Ca_x)Cu_2O_{6+\delta}$, via the sol–gel process combined with the sealed quartz tube method, and bulk superconductivity with a T_c of 85 K has been found in this system. The sol–gel method is better than the SSR in obtaining better purity, chemical homogeneity and chemical reactivity. EDX and powder XRD studies showed that partial Se substitution into the Hg site is found to be very effective in

stabilizing the Sr-based Hg-1212 phase $(Hg_{1-y}Se_y)Sr_2YCu_2O_{6+\delta}$, $y \approx 0.25$. Electrical resistivity and magnetic susceptibility measurements indicated that substitution of Y by Ca is necessary to induce superconductivity in the 1212, $(Hg_{0.75}Se_{0.25})Sr_2(Y_{1-x}Ca_x)Cu_2O_{6+\delta}$ samples. Results of the structural analysis indicate that the O(3) site is four-fold disordered in the $(Hg,Se)O_\delta$ plane. Partial Ca substitution increases the Cu–O(2) apical distance while the buckling angle decreases.

It is evident that the optimized Sr-based (Hg,Se)-1201 and (Hg,Se)-1212 compounds exhibit T_c at around 50 and 85 K, respectively. These results again support the universal feature of the layered cuprate superconductors that the number of the CuO_2 planes in the unit cell is the most important parameter in determining the maximum attainable T_c of a given compound. These Hg/Sr-cuprates are found to be quite stable in an ambient air atmosphere without any degradation of the superconducting properties over a long period.

References

[1] S.N. Putilin, I. Bryntse, E.V. Antipov, Mater. Res. Bull. 26 (1991) 1299.
[2] M. Hervieu, A. Maignan, C. Martin, C. Michel, J. Provost, B. Raveau, J. Solid State Chem. 75 (1988) 212.
[3] J.D. Jorgensen, Phys. Today (1991) 34.
[4] M.A.G. Aranda, Adv. Mater. 6 (1994) 905.
[5] S.N. Putilin, E.V. Antipov, O. Chmaissem, M. Marezio, Nature (London) 362 (1993) 226.
[6] A. Schilling, M. Cantoni, J.D. Guo, H.R. Ott, Nature 363 (1993) 56.
[7] S.N. Putilin, E.V. Antipov, M. Marezio, Physica C 212 (1993) 266.
[8] P.G. Radaelli, J.L. Wagner, B.A. Hunter, M.A. Beno, G.S. Knapp, J.D. Jorgensen, D.G. Hinks, Physica C 216 (1993) 29.
[9] A. Maignan, G. van Tendeloo, M. Hervieu, C. Michel, B. Raveau, Physica C 212 (1993) 239.
[10] A. Maignan, C. Michel, G. van Tendeloo, M. Hervieu, B. Raveau, Physica C 216 (1993) 1.
[11] Z.J. Huang, R.L. Meng, X.D. Qiu, Y.Y. Sun, J. Kulik, Y.Y. Xue, C.W. Chu, Physica C 217 (1993) 1.
[12] O. Chmaissem, Q. Huang, E.V. Antipov, S.N. Putilin, M. Marezio, S.M. Loureiro, J.L. Capponi, J.L. Tholence, A. Santoro, Physica C 217 (1993) 265.
[13] K.A. Lokshin, P.A. Pavlov, S.N. Putilin, E.V. Antipov, D.V. Sheptyakov, A.M. Balagurov, Phys. Rev. B 63 (2001) 64511.
[14] C.W. Chu, L. Gao, F. Chen, Z.J. Huang, R.L. Meng, Y.Y. Xue, Nature 365 (1993) 323.
[15] H. Takahashi, A. Tokiwa-Yamamoto, N. Mori, S. Adachi, H. Yamauchi, S. Tanaka, Physica C 218 (1993) 1.
[16] M. Nunez-Regueiro, J.L. Tholence, E.V. Antipov, J.J. Capponi, M. Marezio, Science 262 (1993) 97.
[17] M. Marezio, J.J. Capponi, P.G. Radaelli, P.P. Edwards, A.R. Armstrong, W.I.F. David, Eur. J. Solid State Inorg. Chem. 31 (1994) 843.
[18] R.S. Liu, S.H. Hu, D.A. Jefferson, P.P. Edwards, Physica C 198 (1992) 318.
[19] M.A. Subramanian, J.B. Parise, J.C. Calabrese, C.C. Torardi, J. Gopalakrishnan, A.W. Sleight, J. Solid State Chem. 77 (1988) 192.
[20] R.S. Liu, S.F. Hu, D.A. Jefferson, P.P. Edwards, P.D. Hunneyball, Physica C 205 (1993) 206.
[21] K.K. Singh, V. Kirtikar, A.P.B. Sinha, D.E. Morris, Physica C 220 (1994) 1.
[22] J. Shimoyama, S. Hahakura, K. Kitazawa, K. Yamafuji, K. Kishio, Physica C 224 (1994) 1.
[23] O. Chmaissem, L. Wessels, Z.Z. Sheng, Physica C 228 (1994) 190.
[24] K. Tang, Y. Qian, Z. Chen, L. Yang, L. Wang, Y. Zhang, Physica C 242 (1995) 216.
[25] O. Chmaissem, Z.Z. Sheng, Physica C 242 (1995) 23;
O. Chmaissem, Z.Z. Sheng, Z. Phys. B 99 (1996) 179.
[26] M. Marezio, F. Licci, Physica C 282 (1997) 53.
[27] E. Kandyel, X.J. Wu, S. Adachi, S. Tajima, Physica C 322 (1999) 9.
[28] D. Polloquin, C. Michel, G. van Tendeloo, A. Maignan, M. Hervieu, B. Raveau, Physica C 214 (1993) 87.
[29] F. Goutenoire, P. Daniel, C. Michel, G. van Tendeloo, A. Maignan, M. Hervieu, B. Raveau, Physica C 216 (1993) 257.
[30] C. Martin, M. Hervieu, M. Huve, C. Michel, A. Maignan, G. van Tendeloo, B. Raveau, Physica C 222 (1994) 19.
[31] M. Hervieu, G. van Tendeloo, A. Maignan, C. Michel, F. Goutenoire, B. Raveau, Physica C 216 (1993) 264.
[32] J.B. Mandal, B. Bandyopadhyay, F. Fauth, T. Chattopadhyay, B. Gosh, Physica C 264 (1996) 145.
[33] K.-B. Tang, X.-W. Xu, Y.-T. Qian, Z.-Y. Chen, L. Yang, Y.-H. Zhang, Physica C 255 (1995) 188.
[34] R.S. Liu, S.F. Hu, D.H. Chen, D.S. Shy, D.A. Jefferson, Physica C 222 (1994) 13.
[35] D. Polloquin, M. Hervieu, C. Michel, G. van Tendeloo, A. Maignan, B. Raveau, Physica C 216 (1993) 257.
[36] K. Tang, Y. Qian, Z. Chen, L. Yang, L. Wang, Y. Zhang, Physica C 248 (1995) 11.
[37] V. Badri, Y.T. Wang, J. Onstad, A.M. Hermann, J. Supercond. 10 (1997) 563.
[38] E. Kandyel, T. Kamiyama, H. Asano, S. Amer, M. Abou-Sekkina, Jpn. J. Appl. Phys. 36 (1997) L6306;
E. Kandyel, T. Kamiyama, H. Asano, M. Abou-Sekkina, Physica C 291 (1997) 97.
[39] E. Kandyel, T. Kamiyama, K. Oikawa, S. Torii, K. Mori, H. Asano, M. Abou-Sekkina, J. Supercond. 13 (1) (2000) 111.
[40] A. Maignan, M. Hervieu, C. Martin, C. Michel, B. Raveau, Physica C 232 (1994) 15.
[41] E. Kandyel, J. Phys. Chem. Solids 64 (2003) 731.
[42] E. Kandyel, Physica C 422 (2005) 102.
[43] S.Y. Li, L. Liu, R. Fan, X.H. Chen, Physica C 356 (2001) 192.
[44] E. Kandyel, X.J. Wu, S. Adachi, S. Tajima, Physica C 319 (1999) 209;
E. Kandyel, X.J. Wu, S. Adachi, S. Tajima, Supercond. Sci. Technol. 12 (1999) 1168.
[45] J. Shimoyama, S. Hahakura, R. Kobayashi, K. Kitazawa, K. Yamafuji, K. Kishio, Physica C 235–240 (1994) 2795.
[46] O. Chmaissem, D.N. Argyrion, D.G. Hinks, J.D. Jorgensen, B.G. Storey, H. Zhang, L.D. Marks, Y.Y. Wang, V.P. Dravid, B. Dabrowski, Phys. Rev. B 52 (1995) 15636.
[47] O. Chmaissem, J.D. Jorgensen, K. Yamaura, Z. Hiroi, M. Takano, J. Shimoyama, K. Kishio, Phys. Rev. B 53 (21) (1996) 14647.
[48] C.J. Brinker, G.W. Scherer, Sol–Gel Science: The Physics and Chemistry of Sol–Gel Processing, Academic Press, New York, 1990.
[49] A. Kareiva, I. Bryntse, J. Mater. Chem. 5 (6) (1995) 885.
[50] Y. Tsabba, S. Reich, Physica C 254 (1995) 21.
[51] S.H. Yoo, K.W. Wong, Y. Xin, Physica C 273 (1997) 189.
[52] K. Knizek, M. Verveka, E. Hadova, J. Hejtmanek, D. Sedmidubsky, E. Pollert, Physica C 302 (1998) 290.
[53] G.B. Peacock, A. Asab, J.P. Hodges, I. Gameson, P.P. Edwards, Physica C 235–240 (1994) 911.
[54] E. Kandyel, K. Elsabawy, Physica C (2008), in press, doi:10.1016/j.physc.2008.08.009.
[55] Y.-I. Kim, F. Izumi, J. Ceram.Soc. Jpn. 102 (1994) 401.
[56] R.D. Shannon, Acta Crystallogr. A 32 (1976) 751.
[57] R. Vijayaraghavan, N. Rangavittal, G.U. Kulkarni, Physica C 179 (1991) 183.
[58] Neil C. Hyatt, Ian Gameson, Kelly L. Moran, Ray Dupree, Physica C 391 (2003) 160.
[59] A. Fukuoka, A. Tokiwa-Yamamoto, M. Itoh, R. Usami, S. Adachi, K. Tanabe, Phys. Rev. B 55 (1997) 6612.